

**DRAFT: A PHYSICALLY MOTIVATED INTERNAL STATE VARIABLE PLASTICITY
AND DAMAGE MODEL EMBEDDED WITH A LENGTH SCALE FOR HAZMAT TANK
CARS' STRUCTURAL INTEGRITY APPLICATIONS**

Fazle R. Ahad *
MSU/CAVS

Starkville, Mississippi 39759
Email: fra11@cavs.msstate.edu

Koffi Enakoutsa
MSU/CAVS

Starkville, Mississippi 39759
Email: koffi@cavs.msstate.edu

Kiran N. Solanki
MSU/CAVS

Starkville, Mississippi 39759
Email: kns3@cavs.msstate.edu

Yustianto Tjipowidjojo
MSU/CAVS

Starkville, Mississippi 39759
Email: yusti@cavs.msstate.edu

Douglas J. Bammann
MSU/CAVS

Starkville, Mississippi 39759
Email: bammann@cavs.msstate.edu

ABSTRACT

In this study, we use a physically-motivated internal state variable model containing a mathematical length scale to represent the material behavior in finite element (FE) simulations of hazmat tank car shell impacts. Two goals motivated the current study: (1) to reproduce with high fidelity finite deformation and temperature histories, damage, and high rate phenomena which arise during the impact, as well as (2) to investigate numerical aspects associated with post-bifurcation mesh-dependency of the finite element solution. We add the mathematical length scale to the model by adopting a nonlocal evolution equation for the damage, as suggested by Pijaudier-Cabot and Bazant (1987) in a slightly different context. The FE simulations consist of a moving striker colliding against a stationary hazmat tank car and are carried out with the aid of ABAQUS/Explicit. The results of these simulations show that accounting for temperature histories and nonlocal damage effects in the material model satisfactorily predicts, independently of the mesh size, the failure process of the tank car impact accident.

1 INTRODUCTION

The design of accident-resistant hazmat tank cars requires material models which describe the physical mechanisms that occur during an accident. In the case of high-velocity impact accidents, finite deformation and temperature histories, damage and high rate phenomena are generated in the vicinity of the impact damage zone. Unfortunately, the majority of material models used in the finite element simulation of hazmat tank car impact scenarios do not account for such physical features. Furthermore, in the few models that do, a mathematical length scale aimed at solving the post-bifurcation problem is absent. As a consequence, when one material point fails, the boundary value problem for such material models changes, from a hyperbolic to an elliptical system of differential equations in dynamic problems, and the reverse in statics. In both cases, the boundary value problem becomes ill-posed (Muhlhaus (1986), Tvergaard and Needleman (1997), de Borst (1993), Ramaswamy and Aravas (1998)), as the boundary and initial conditions for one system of differential equations are not suitable for the other. As a result, bifurcations with an infinite number of bifurcated branches appear, which raises the problem of selecting the relevant one, especially in numerical computations where this drawback manifests itself as a pathological sensitivity of the results to the finite

*Address all correspondence to this author.

element discretization.

Alternatively to the shortcomings encountered in hazmat tank car impacts' numerical simulations, we propose to use a nonlocal version of the BCJ¹ model (Bammann and Aifantis (1987) and Bammann et al. (1993)), a physically-motivated internal state variable plasticity and damage model containing a mathematical length scale. The use of internal state variables will enable the prediction of strain rate and temperature histories effects. These effects can be quite substantial and therefore difficult to incorporate into material models, which assumes that the stress is (1) a unique function of the current strain, strain rate and temperature and (2) is independent of the loading path. The effects of damage are included in the BCJ model, however, through a scalar internal state variable which tends to degrade the elastic moduli of the material as well as to concentrate the stress. The mathematical length scale is introduced in the model via the nonlocal damage approach of Pijaudier-Cabot and Bazant (1987). In the context of concrete damage, these authors suggested a formulation in which only the damage variable is nonlocal, while the strain, the stress and other variables retain their local definition. Their formulation has been applied to creep problems by Saanouni et al. (1989) and extended to plasticity by, among others, Leblond et al. (1994) and Tvergaard and Needleman (1995). Following Pijaudier-Cabot and Bazant (1987)'s suggestion, a nonlocal evolution equation for the damage within an otherwise unmodified BCJ model is adopted in the current study. The time-derivative of the damage is expressed as the spatial convolution of a "local damage rate" and bell-shaped weighting function. The width of this function introduces a mathematical length scale.

In this study, a dynamic nonlinear finite element analysis, carried out with ABAQUS/Explicit finite element code, is used to simulate a moving striker colliding against a stationary hazmat tank car. The structure part of this finite element model is represented by Lagrangian elements obeying the nonlocal version of the BCJ model, while the fluid part is represented by Eulerian elements. The objective of this study is two-fold: (1) use a high fidelity material model to idealize the physics occurring during the impact accident and (2) rectify the computational drawback (post-bifurcation mesh dependence issues) for this model on a large-scale boundary value problem. The resulting numerical simulations of hazmat tank car impact scenarios, which account for nonlocal damage and temperature history effects predict satisfactorily the tank car failure process independently of the element size. The originality of this work lies in that, prior to this study², never have the post-bifurcation mesh dependence issues been investigated on large-scale computations problems for steels. The paper is organized as follows:

Section 1 describes the physics associated with the failure

process of a hazmat tank car impact accident.

Section 2 provides a summary of the equations of the BCJ model and its nonlocal extension.

Section 3 discusses several methods to numerically implement the integral-type nonlocal damage into existing ABAQUS finite element BCJ model subroutines. The main difficulty encountered in this implementation relates to the double loop over the integration points required by the calculation of several convolution integrals, which might otherwise dismantle the architecture of the entire code.

Finally Section 4 is devoted to numerical applications of the local and nonlocal BCJ model on hazmat tank car shell impact accident simulations.

2 PHYSICS OF THE DAMAGE FROM HAZMAT TANK CAR IMPACT

The physical mechanisms responsible for the damage to hazmat tank cars during high-velocity impact initiates at the time of the contact, wherein strong pressure waves arise and propagate along both the striker and the hazmat tank car. During this propagation, hydrostatic compression and tension shock waves evolve and can lead to so-called spalling fracture. Spalling fracture occurs when the shock waves produced by the impact bounce off the back surface of the tank car, reverse direction, and return as reflected tensile waves (see Zukas (1990)). When these tensile waves exceed the local spall strength, nucleation, growth, and coalescence of voids and/or cracks may occur. These defects then lead to the tank car's failure: usually, a chunk of material breaks away from the surface opposite to impacted surface.

The propagation of the shock waves is also accompanied by a quick local heating due to the intense plastic shear deformations and the passage of shock waves. Heat is generated rapidly such that little conduction occurs and hence the process is adiabatic. As a result, material softening occurs in the impact region, while the surrounding material continues to harden; also, the deformation in the local damaged zone is nonuniformly distributed in narrow adiabatic shear bands (Glema et al. (2000)). While these bands do not deteriorate the hazmat tank car structural integrity as cracks do, they are typically precursors to fracture. The BCJ model is capable of representing with high fidelity the strain rate, temperature history, load path, and damage effects which arise during the impact accident. This model is presented in the next section.

3 THE BCJ MODEL CONTAINING A MATHEMATICAL LENGTH SCALE

3.1 THE BCJ MODEL

The BCJ model is a physically-based plasticity model coupled with the Cocks and Ashby (1980)'s void growth failure model. The BCJ model incorporates load path, strain rate, and

¹BCJ: Bammann-Chiesa-Johnson

²To the best of the authors' knowledge.

temperature history effects, as well as damage through the use of scalar and tensor internal state variables for which the evolution equations are motivated by dislocation mechanics and cast in a hardening minus-recovery format. The BCJ model also accounts for deviatoric deformation resulting from the presence of dislocations and dilatational deformation.

The deformation gradient is multiplicatively decomposed into terms that account for the elastic, deviatoric inelastic, dilatational inelastic, and thermal inelastic parts of the motion. For linearized elasticity, the multiplicative decomposition of the deformation gradient results in an additive decomposition of the Eulerian strain rate into elastic, deviatoric inelastic, dilatational inelastic, and thermal inelastic parts. The constitutive equations of the model are written with respect to the intermediate (stress free) configuration defined by the inelastic deformation such that the current configuration variables are co-rotated with the elastic spin. The pertinent equations of the BCJ model are expressed as the rate of change of the observable and internal state variables and consist of the following elements.

- A hypoelasticity law connecting the elastic strain rate to an objective time-derivative Cauchy stress tensor is given by:

$$\dot{\tilde{\sigma}} = \lambda(1 - \phi)\text{tr}(\mathbf{D}^e)\mathbf{I} + 2\mu(1 - \phi)\mathbf{D}^e - \frac{\dot{\phi}}{1 - \phi}\boldsymbol{\sigma}, \quad (1)$$

³ where λ is the Lamé constant, μ is the shear modulus, and ϕ denotes the damage variable. The Cauchy stress $\boldsymbol{\sigma}$ is convected with the elastic spin \mathbf{W}^e as

$$\dot{\tilde{\sigma}} = \dot{\boldsymbol{\sigma}} - \mathbf{W}^e\boldsymbol{\sigma} + \boldsymbol{\sigma}\mathbf{W}^e \quad (2)$$

where, in general, for any arbitrary tensor variable \mathbf{X} , $\dot{\tilde{\mathbf{X}}}$ represents the convective derivative. Note that the rigid body rotation is included in the elastic spin; therefore, the constitutive model is expressed with respect to a set of directors whose direction are defined by the plastic deformation.

- The decomposition of both the skew symmetric and symmetric parts of the velocity gradient into elastic and inelastic parts for the elastic stretching rate \mathbf{D}^e and the elastic spin \mathbf{W}^e in the absence of elastic-plastic couplings yields

$$\begin{cases} \mathbf{D}^e = \mathbf{D} - \mathbf{D}^p - \mathbf{D}^d - \mathbf{D}^{\text{th}} \\ \mathbf{W}^e = \mathbf{W} - \mathbf{W}^p. \end{cases} \quad (3)$$

³Strictly speaking, additional terms containing the temperature θ and its derivatives should be added to Eqn.1. The influence of the additional terms, however, is significant only for problems involving very high temperatures, such as welding problems; therefore we can safely ignore them here.

Note that for problems in the shock regime, only the deviatoric elastic strain part is linearized enabling prediction of large elastic volume changes.

- Next, the equation for the plastic spin \mathbf{W}^p is introduced, in addition to the flow rules for \mathbf{D}^p and \mathbf{D}^d , and the stretching rate due to the unconstrained thermal expansion \mathbf{D}^{th} . From the kinematics, the dilatational inelastic \mathbf{D}^d flow rule is given as:

$$\mathbf{D}^d = \frac{\dot{\phi}}{1 - \phi}\mathbf{I}. \quad (4)$$

Assuming isotropic thermal expansion, the unconstrained thermal stretching rate \mathbf{D}^{th} can be expressed by

$$\mathbf{D}^{\text{th}} = A\dot{\theta}\mathbf{I}, \quad (5)$$

where A is a linearized expansion coefficient.

For the plastic flow rule, a deviatoric flow rule (Bammann (1988)) is assumed and defined by

$$\mathbf{D}^p = f(\theta)\sinh\left[\frac{\|\boldsymbol{\sigma}' - \boldsymbol{\alpha}\| - [\kappa - Y(\theta)](1 - \phi)}{V(\theta)(1 - \phi)}\right] \frac{\boldsymbol{\sigma}' - \boldsymbol{\alpha}}{\|\boldsymbol{\sigma}' - \boldsymbol{\alpha}\|}, \quad (6)$$

where θ is the temperature, κ the scalar hardening variable, $\dot{\tilde{\alpha}}$ the objective rate of change of $\boldsymbol{\alpha}$, the tensor hardening variable, and $\boldsymbol{\sigma}'$ the deviatoric Cauchy stress.

There are several choices for the form of \mathbf{W}^p . The assumption $\mathbf{W}^p = 0$ allows recovery of the Jaumann stress rate. Alternatively, this function can be described by the Green-Naghdy rate of Cauchy stress. We used the Jaumann rate for the numerical applications in this paper.

- The evolution equations for the kinematic and isotropic hardening internal state variables are given in a hardening minus recovery format by

$$\begin{cases} \dot{\tilde{\alpha}} = h(\theta)\mathbf{D}^p - \left[\sqrt{\frac{2}{3}}r_d(\theta)\|\mathbf{D}^p\| + r_s(\theta)\right]\|\boldsymbol{\alpha}\|\boldsymbol{\alpha} \\ \dot{\kappa} = H(\theta)\|\mathbf{D}^p\| - \left[\sqrt{\frac{2}{3}}R_d(\theta)\|\mathbf{D}^p\| + R_s(\theta)\right]\kappa^2, \end{cases} \quad (7)$$

where h and H are the hardening moduli, r_s and R_s are scalar functions of θ describing the diffusion-controlled ‘‘static’’ or ‘‘thermal’’ recovery, and r_d and R_d are the functions of θ describing dynamic recovery.

- To describe the inelastic response, the BCJ model introduces nine functions which can be separated into three groups. The first three are the initial yield, the hardening, and the recovery functions, defined as

$$\begin{cases} V(\theta) = C_1 \exp(-C_2/\theta) \\ Y(\theta) = C_3 \exp(-C_4/\theta) \\ f(\theta) = C_5 \exp(-C_6/\theta). \end{cases} \quad (8)$$

The second group is related to the kinematic hardening process and consists of the following functions:

$$\begin{cases} r_d(\theta) = C_7 \exp(-C_8/\theta) \\ h(\theta) = C_9 \exp(-C_{10}/\theta) \\ r_s(\theta) = C_{11} \exp(-C_{12}/\theta). \end{cases} \quad (9)$$

The last group is related to the isotropic hardening process and is composed of

$$\begin{cases} R_d(\theta) = C_{13} \exp(-C_{14}/\theta) \\ H(\theta) = C_{15} \exp(-C_{16}/\theta) \\ R_s(\theta) = C_{17} \exp(-C_{18}/\theta). \end{cases} \quad (10)$$

In Eqns. (8, 9, 10), C_i is some parameter of the model which need to be determined.

- The evolution equation for damage, credited to Cocks and Ashby (1980), is given by

$$\dot{\phi} = \left[\frac{1}{(1-\phi)^n} - (1-\phi) \right] \sinh \left[\frac{(1-n) \mathcal{P}}{(1+n) \bar{\sigma}} \right] \| \mathbf{D}^p \| . \quad (11)$$

Note that this void growth model displays a “sinh”-dependence on the triaxiality factor $\mathcal{P}/\bar{\sigma}$, as well as an additional parameter n along with the initial value of the damage ϕ_0 required to calculate damage growth.

- The last equation to complete the description of the model is one that computes the temperature change during high strain rate deformations, such as those encountered in high rate impact loadings. For these problems, a non-conducting (adiabatic) temperature change following the assumption that 90% of the plastic work is dissipated as heat is assumed. Taylor and Quinney (1934) were the first to measure the energy dissipation from mechanical work as being between 5 – 50% of the total work for various materials and strain levels. Therefore, the rate of the change of the temperature is assumed to follow

$$\dot{\theta} = \frac{0.9}{\rho C_v} (\sigma \mathbf{D}^p), \quad (12)$$

where ρ and C_v represent the material density and a specific heat, respectively.

The empirical assumption in Eqn.(12) has permitted non-isothermal solution by finite element that is not fully coupled with the energy balance equation (see Bammann et al. (1993)). Note that the temperature rise will induce a profound effect on the constitutive behavior of the material. Specifically, the temperature increase will lead to thermal softening (adiabatic shear bands), and as a result shear instabilities may arise. The model is also suitable to predict mechanical softening through a gradual increase of the damage. It is well known that practical finite element applications of constitutive models involving softening, like the BCJ model, are strongly mesh-dependent. According to Rousselier (1981), this problem can be obviated by putting a lower limit on the element size. However, this practice is not optimal theoretically. Another, more elaborated, solution consists of including a mathematical length scale in these constitutive models. The following section presents a technique to embed the BCJ model with just such a mathematical length scale.

3.2 EMBEDDING A LENGTH SCALE IN THE BCJ MODEL

Following Pijaudier-Cabot and Bazant (1987)’s suggestion in the context of concrete damage, we propose to delocalize the variable(s) responsible for softening. In the BCJ model, softening may arise from two mechanisms: a gradual increase of the damage (under isothermal conditions) or a temperature rise (in adiabatic conditions) followed by an increase of the damage. While temperature and damage parameters seem to govern softening in adiabatic conditions, review of the model’s constitutive equations provided in the previous section reveals that these two variables are related. We choose to introduce the length scale on the damage evolution equation. This choice appears quite appealing from the physical point of view. Indeed, in the case of heterogeneous materials, for example, the damage can only be defined by considering “elementary” volumes of size greater than the voids spacing⁴ and is therefore a nonlocal quantity.

The evolution equation of this variable is given by a convolution integral including a bell-weighting function the width of which introduces a mathematical length scale:

$$\dot{\phi}(x) = \frac{1}{B(x)} \int_{\Omega} \dot{\phi}^{\text{loc}}(y) A(x-y) d\Omega_y. \quad (13)$$

In this equation, Ω denotes the volume studied, and A the Bell weight function defined as

$$A(x) = \exp(- \| x \|^2 / l^2), \quad (14)$$

⁴The Cocks and Ashby (1980) void growth model is based on a cylinder containing a spherical void.

where l is the mathematical length scale. The factor $B(x)$ and the “local damage rate $\dot{\phi}^{loc}$ ” are given by

$$B(x) = \int_{\Omega} A(x-y)d\Omega_y \quad (15)$$

and Eqn.(11), respectively. The function A is indefinitely differentiable and does not introduce any Dirac’s δ -distribution at the point 0. This means that the function $\dot{\phi}$ is not partially local but entirely nonlocal. The function A is also isotropic and normalized. The point here is that $\dot{\phi}$ must be equal to $\dot{\phi}^{loc}$ if the latter variable is spatially uniform. This would not be the case near the boundary of Ω in the absence of the normalization factor $1/B$. The presence of this term allows for the coincidence everywhere.

The new evolution equation for the damage, Eqn.(13), along with the equation for the temperature rise, Eqn.(12), should predict satisfactorily the failure process of the tank car impact independently of the mesh size. Indeed, the local damage rate Eqn.(13) implicitly depends on the temperature through the strain rate sensitivity parameter (see Eqn.(6) and Yamaguchi et al. (1992)). When the temperature gradually rises, which is the case in high-velocity impact loadings, the damage rate in this zone quickly climbs to a high value; as a result, the damage grows rapidly to reach the critical failure damage. The convolution integral in Eqn.(13) enhances the rapid damage increase, since it involves the sum of several positive terms each of which contains a local damage velocity. The mathematical length scale in the convolution integral eliminates the mesh sensitivity effects.

Nonetheless, the numerical implementation of the new evolution equation for the damage rate into an existing finite element code is not an easy task because of the double loop over integration points required by the calculation of several convolution integrals, which may potentially compromise the entire architecture of the existing code. The following section is devoted to explaining this implementation.

4 NUMERICAL TREATMENT OF THE NONLOCAL DAMAGE RATE

The numerical implementation of the original BCJ model into a finite element code such as ABAQUS has been extensively addressed in Bammann et al. (1993); consequently, it will not be repeated here. Recall, however, that this implementation is based on Krieg and Krieg (1977)’s radial return method to solve numerically the equations presented in Section 3.1 for the deviatoric stresses, equivalent plastic strain, pressure, temperature, and damage at each new time-step. The algorithm is available in both the implicit and explicit versions of ABAQUS.

To implement the nonlocal damage rate in the implicit version of the code, we have computed the nonlocal damage increment at convergence by means of the subroutine URDFIL, which

stores all the variables necessary for the convolution operation, performs this operation, and stores the nonlocal damage increment for all the integration points involved in the finite element model. The nonlocal damage increment is used to calculate the damage at time $t + \Delta t$ for the next time-step following the formula:

$$\phi(t + \Delta t) \approx \phi(t) + \dot{\phi}(t)\Delta t. \quad (16)$$

This updated value is an explicit estimation of the damage at $t + \Delta t$ and is not used to repeat the whole process of solution between times t and $t + \Delta t$. Thus, the algorithm is not fully implicit, but mixed implicit/explicit. Enakoutsa et al. (2007) used the same technique to implement a nonlocal version of Gurson (1977)’s model following a slightly modified Aravas (1987)’s algorithm, the so-called “projection into the yield surface” algorithm. The explicit nature of Enakoutsa et al. (2007)’s algorithm with respect to the damage allowed these authors to prove that the *projection problem* associated with Gurson’s nonlocal model has a unique solution. The latter property is a direct consequence of the fact that the constitutive equations of Gurson’s nonlocal model belong to the class of Generalized Standard Materials of Halphen and Nguyen (1975). Applications of the numerical treatment of nonlocal damage rate on a double-notched edge specimen in tension problem (see Fig.1) illustrate the validity of the method to avoid ill-posed issues in this laboratory-oriented boundary value problem. Indeed, while the local BCJ model concentrates the damage within a layer of meshes between the specimen notches, the nonlocal BCJ model spreads the damage region to a zone beyond this layer.

To assess the validity of the method to regularize hazmat tank car impact boundary value problems requires implementation of the nonlocal damage rate in the explicit version of the BCJ model VUMAT subroutine. One option of doing so consists of branching outside the “NBLOCK loop” in the VUMAT, which allows the computation of the nonlocal damage rate at each integration point using the coordinates, the local damage velocities, and the weights of “NBLOCK” integration points. This method also successfully avoids the localization problems arising in the numerical simulations of double-notched edge specimen tensile tests and therefore is expected to reduce, if not completely remove, the mesh-sensitivity issues arising in the hazmat tank car impacts numerical simulations.

5 HAZMAT TANK CAR SHELL IMPACT FE SIMULATIONS

The goal of the hazmat tank car shell impact FE simulations is to virtually predict the tank car structural’s failure process independently of the element size. To that end, we describe the impact accident physical problem, the associated FE model in

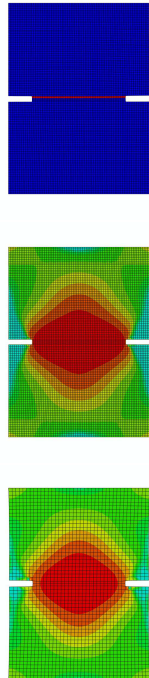


Figure 1. Comparison of the damage distribution of a double-notched edge specimen tensile tests for local and nonlocal BCJ models. Note the localization of the damage in a row of meshes between the two notches for the local BCJ model (top) and the similarity between the damage pattern of two different meshes for the nonlocal BCJ model (middle and bottom).

ABAQUS, and we present different numerical predictions of the damage created by the impact.

5.1 PROBLEM DEFINITION

The previous work of Tang et al. (2008a) and Tang et al. (2008b) inform the current problem. In our study, a ram car weighing 286,000 pounds and with a protruding beam to which an impactor was attached, is moving horizontally at 10 m/s into an immobile hazmat tank car. Fifty percent of the tank car is filled with water mixed with clay slurry, which together has the approximate density of liquid chlorine. Air occupied the remaining volume in the tank car and is pressurized 100 psi. The impactor used in the problem is conical sharp-nose shaped (see Fig.2); it is introduced in the FE model to generate a ductile failure mode during the impact. The stationary part of the problem consists of a tank car surrounded by a jacket. The tank is a 0.777-inch-thick cylinder, and closed at its two ends with elliptical caps of aspect ratio 2. The tank body material consists of 304L stainless steel; the jacket is a 0.119-inch-thick made of the same steel. A 4-inches-thick layer separates the jacket from the tank car. This layer is introduced to account for insulation and



Figure 2. Geometry of the conical impactor used in the simulations. The sharp nose is used to generate a ductile failure mode of the tank car during the impact.

thermal protection between the tank car and the jacket. The entire assembly (Tank/Layer/Jacket) is supported by two rigid legs and this assembly is placed with one side against a rigid wall and the other side exposed to impact from the impactor.

5.2 FE MODEL OF THE PROBLEM IN ABAQUS

The FE model of the problem consists of an Eulerian mesh representing the fluid in the tank car and a Lagrangian mesh idealizing the tank, the jacket, and the impactor. The impactor consists of R3D4 rigid elements, while the tank and the jacket are meshed using solid C3D8R elements. For the sake of simplicity, the space between the tank and the jacket is assumed to be empty. The two legs are rigid and are idealized with squared analytical surfaces on which reference points located below the jacket are assigned. Each reference point is kinematically coupled with a definite set of nodes on the jacket and the tank car. The contact algorithm available in the 6.10 version of ABAQUS/Explicit finite element code is used to account for all possible contacts between different parts in the model.

The Eulerian mesh is based on the volume-of-fluid (VOF) method. The VOF method (widely used in Computational Fluid Dynamics) tracks and locates the fluid free surface; it belongs to the class of Eulerian methods that are characterized by either a stationary or moving mesh. The VOF method suitably captures the change of the fluid interface topology. In this method, the material in each element is tracked as it flows through the mesh using the Eulerian volume fraction (EVF), a unique parameter for each element and each material.

The material parameters are determined from tension, compression and torsion tests under different constant strain rate and temperatures. We used the material parameters provided in Horstemeyer et al. (2000).

5.3 SIMULATIONS RESULTS

This section presents evidence of the integral-nonlocal damage method's to eliminate mesh-dependence issues which arise in the FE solution of hazmat tank car impact accident problems.

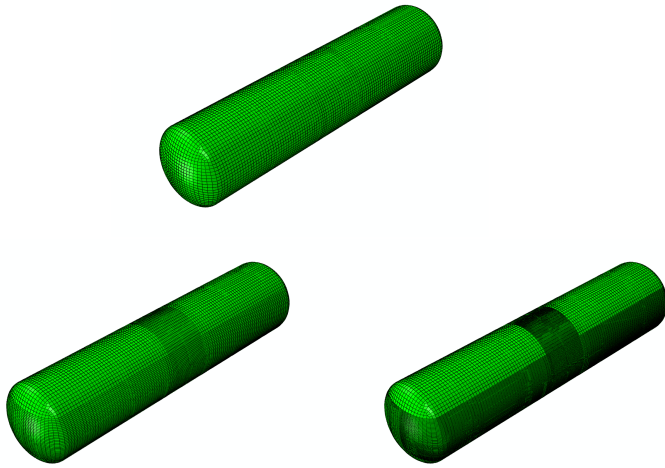


Figure 3. Meshes of the tank car. Top: coarse mesh, bottom-left: medium mesh, bottom-right: fine mesh. The meshes are made of solid C3D8R elements.

To that end, the calculations were performed on three different meshes, a coarse, medium, and fine mesh (see Fig.3), for the local and nonlocal versions of the BCJ model in adiabatic conditions. In isothermal conditions, the BCJ model difficultly predicts failure (see Bammann et al. (1993)); therefore, isothermal conditions are not considered here.

Figure 4 illustrates the repartition of damage on the inner surface of the tank for all three meshes at the same time, in the case of the local BCJ model. The choice to show only the repartition of the damage on the inner surface of the tank but not on the outer surface is noteworthy. The damage mechanism during the impact accident suggested in Section 2 supposes that the side opposite from the impact surface may fail first. This observation agrees well with Bammann et al. (1993)'s simulations of a thin circular plate impact in which damage initiation and propagation indeed occurs on the opposite side of the impact surface. Thus, it is expected that the effect of nonlocal damage will be significant at that place.

The results of the simulations using the local BCJ model are mesh-dependent: the pattern of the damage is determined by the size of the elements. Therefore, decreasing of FE size will modify the global response of the structure (which depends explicitly on the number of elements). Furthermore, the energy generated during the impact tends to zero when the size of the FE approaches zero. This leads to the meaningless conclusion that the tank car fails during the accident with zero energy dissipated. In fact, the FE solutions depend not only on the size of the elements, but on their nature, orientation, degree of interpolation function-in short, on the finite elements approximation space, as presented in Darve et al. (1995).

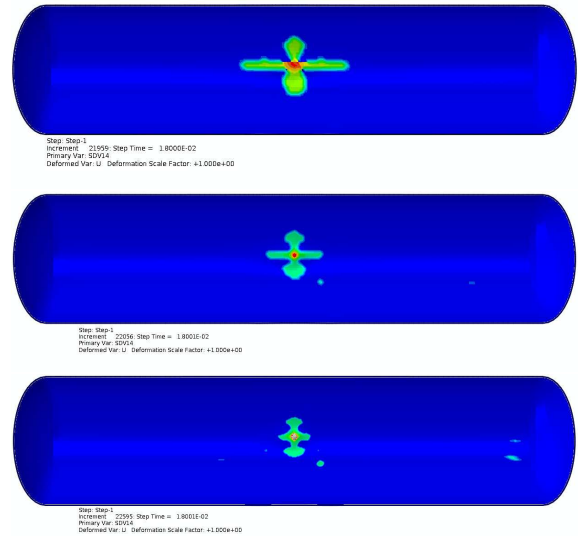


Figure 4. An illustration of the mesh size effects in the FE simulations of hazmat tank car using the local BCJ model. The figure shows the damage pattern on the inner surface of the tank located behind the impact region for a coarse (top), medium (middle), and fine (bottom) mesh at the same time. Note the reduction of the damage pattern size with decreasing element size.

Figure.5 is the analogous of Fig.4. Here, the pattern of the damage for the three meshes is relatively similar; this observation holds for a latter time, as displayed in Fig.6. The similarity would be more significant if a very refined mesh were used because, as in the case of local BCJ model, the element size determines the damage pattern. Thus, the nonlocal damage rate, and *a fortiori* the damage itself, has a significant influence on the response of the hazmat tank car to the impact loading.

Also remarkable from Figs.(5, 6) are the bands, which do appear in the local simulations, seem to have almost completely disappeared. In fact, the nonlocal damage has delayed their apparition to latter times where these bands are extended over several elements. This postponement arises because the damage in the bands is much larger at latter stages of the impact loading, due to the progressive development of considerable stress in this zone.

6 SUMMARY AND RECOMMENDATION

With the aid of ABAQUS/Explicit FE code, we have presented a dynamic nonlinear FE simulations of a hazmat tank car shell impact. In these simulations, the tank car body material was idealized with a physically-motivated internal state variable model containing a mathematical length scale, the nonlocal BCJ model. This model consists of all the constitutive equations of the original BCJ model, except the evolution equation for the

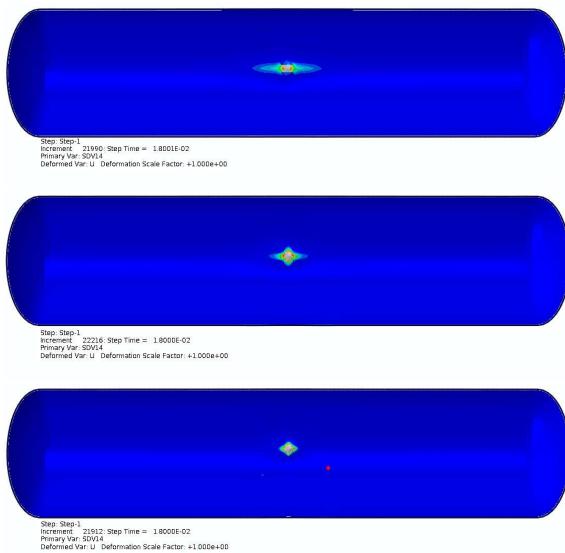


Figure 5. An illustration of the introduction of the mathematical length scale in the BCJ model to reduce the mesh size effects in the FE simulations of hazmat tank car. The contour plots of the damage on the inner face of the tank are shown for three different meshes at the same time as in Fig.4: coarse (top), medium (middle), and fine (bottom). Note the similarity of the damage pattern size for the three meshes.

damage, which is modified into a nonlocal one. Numerical methods to implement this equation in existing BCJ model subroutines were also presented.

The results of the simulations show the ability of the mathematical length scale to eliminate the pathological mesh-dependency issues while predicting satisfactory hazmat tank car impact failure, provided that nonlocal damage effects are coupled with temperature history effects (adiabatic effects). Thus, the nonlocal BCJ model is a powerful tool that we recommend hazmat tank car fabrication industries incorporate in their virtual design tools.

ACKNOWLEDGMENTS

The study was supported by the U.S. Department of Transportation, Office of the Secretary, Grant No. DTOS9-08-G-00103. Dr. Esteban Marin and Mrs. Clémence Bouvard are gratefully thanked for their insightful discussions on the topic.

REFERENCES

[Aravas (1987)] Aravas N. 1987. "On the Numerical Integration of a Class of Pressure-dependent Plasticity Models," *Int. J. Num. Meth. Engng.*, **24**, 1395-1416.

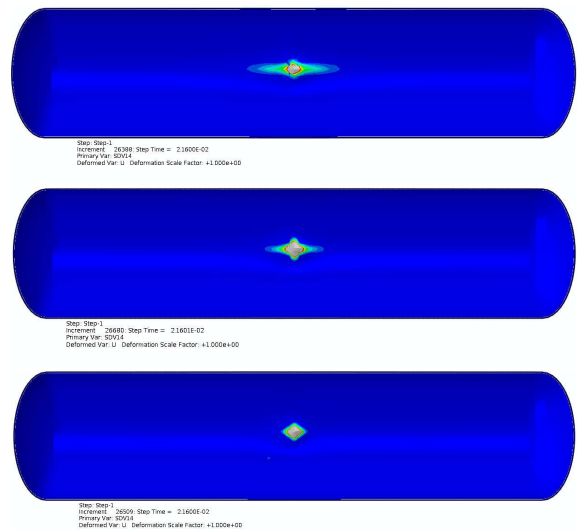


Figure 6. Another illustration of the mathematical length scale effects in the hazmat tank car FE simulations. The contour plots of the damage pattern on the inner surface on the tank are shown for a time greater the one in Figs.(4, 5). Note here also the similarity between the damage pattern.

[Bammann et al. (1993)] Bammann D. J., Chiesa M. L., Horstemeyer, M. F., and Weingarten, L. I., 1993. "Failure in Ductile Materials using Finite Element Methods," *Structural Crashworthiness and Failure*, N. Jones, T. Wierzbicki, ed., Elsevier Applied Science, New York, 1993, pp.1-54.

[Bammann (1988)] Bammann, J.D., 1988. "Modelling the Large Strain-High Temperature Response of Metals," in *Modeling and Control of Casting and Welding Process IV*, eds. Giamei, A.F. and Abbaschian, G.J. TMS Publications, Warrendale, PA.

[Bammann and Aifantis (1987)] Bammann, D.J. and Aifantis, E.C., 1987. "A Model for Finite-deformation Plasticity", *Acta. Mech.*, **69**, 97-117.

[de Borst (1993)] de Borst, R., 1993. "Simulation of Strain Localization: a Reappraisal of the Cosserat Continuum," *Eng. Comput.*, **8**, 317-332.

[Cocks and Ashby (1980)] Cocks, A.C.F. and Ashby, M.G., 1980. "Intergranular Fracture During Power-Law Creep under Multiaxial Stresses," *Metal Science*, Aug-Sept, pp. 395-402.

[Darve et al. (1995)] Darve, F., Hicher, P.-Y., Reynouard J.M., 1995. "Mécanique des Géomatériaux," Hermès, Paris.

[Enakoutsa et al. (2007)] Enakoutsa K., Leblond J.B. and Perrin G., 2007. "Numerical Implementation and Assessment of a Phenomenological Nonlocal Model of Ductile Rupture," *Comput. Meth. Appl. Mech. Engng.*, **196**, 1946-1957.

[Glema et al. (2000)] Glema, A., Lodygowski, T., and Perzyna, P., 2000. "interaction of deformation Waves and Localiza-

- tion Phenomena in Inelastic Solids,” *Comput. Methods Appl. Mech. Engrg.*, **183**, pp. 123-140.
- [Guo et al. (2005)] Guo, Y.B., Wen, Q., and Horstemeyer, M. F., 2005. “An Internal State Variable Plasticity-based Approach to Determine Dynamic Loading History Effects on Material Property in Manufacturing Processes,” *Int. Journal of Mechanical Sciences*, **47**, 1423-1441.
- [Gurson (1977)] Gurson A.L. 1977. “Continuum Theory of Ductile Rupture by Void Nucleation and Growth: Part I - Yield Criteria and Flow Rules for Porous Ductile Media,” *ASME J. Engng. Materials Technol.*, **99**, 2-15.
- [Halphen and Nguyen (1975)] Halphen B. and Nguyen Q.S., 1975. “Sur les Matériaux Standards Généralisés,” *Journal de Mécanique*, **14**, 39-63, in French.
- [Horstemeyer et al. (2000)] Horstemeyer, M.F., Matalanis, M.M., Siebe, M.L., 2000. “Micromechanical Finite Element Calculations of Temperature and Void Configuration Effects on Void Growth and Coalescence,” *international Journal of Plasticity*, **16**, pp. 979-1015.
- [Johnson (1987)] Johnson, W., 1987. “Henri Tresca as the Originator of Adiabatic Heat Lines”, *Int. J. Mech. Sci.*, **29**, pp. 301-310.
- [Krieg and Krieg (1977)] Krieg R.D., and Krieg D.B., 1977. “Accuracies of Numerical Solution Methods for the Elastic-Perfectly Plastic Model,” *ASME Pressure Vessel Tech.*, **99**, 510.
- [Leblond et al. (1994)] Leblond, J.B., Perrin, G., and Devaux, J., 1994. “Bifurcation Effects in Ductile Metals with Nonlocal Damage”, *ASME J. Applied. Mech.*, **61**, 236-242.
- [Muhlhaus (1986)] Muhlhaus, H.-B., 1986. “Shear Band Analysis in Granular Materials by Cosserat Theory,” *Ing. Arch.*, **56**, 389-399.
- [Pijaudier-Cabot and Bazant (1987)] Pijaudier-Cabot, G. and Bazant, Z.P., 1987. “Nonlocal Damage Theory”, *ASCE J. Engrg. Mech.*, **113**, 1512-1533.
- [Ramaswamy and Aravas (1998)] Ramaswamy, S. and Aravas, N., 1998. “Finite Element Implementation of Gradient Plasticity Models part I: Gradient-dependent Yield Functions,” *Mech. Eng.*, **163**, pp. 11-32.
- [Saanouni et al. (1989)] Saanouni, K., Chaboche, J.L. and Lesne, P.M., 1989. “On the Creep Crack-growth Prediction by a Nonlocal Damage Formulation,” *European Journal of Mechanics A/Solids*, **8**, pp. 437-459.
- [Tang et al. (2008a)] Tang, Y.H., Yu, H., Gordon, J.E., Jeong, D.Y., and Perlman, A.B., 2008. “Analyses of Railroad Tank Car Shell Impacts Using Finite Element Method,” *Proceedings of the 2008 IEEE/ASME Joint Rail Conference*, JRC2008-63014.
- [Tang et al. (2008b)] Tang, Y.H., Yu, H., Gordon, J.E., Jeong, D.Y., 2008. “Finite Element Analyses of Railroad Tank Car Head Impacts,” *Proceedings of the 2008 ASME Rail Transportation Division Fall Technical Conference*, RTDF2008-74022.
- [Taylor and Quinney (1934)] Taylor, G.I., and Quinney, H., 1934. “The Latent Energy Remaining in a Metal after Cold Working,” *Proc. Roy. Lond. Soc.*, Vol. A145.
- [Tvergaard and Needleman (1997)] Tvergaard, V. and Needleman, A., 1997. “Nonlocal Effects on Localization in a Void-sheet,” *Int. J. Solids and Struct.*, **34**, pp. 2221-2238.
- [Tvergaard and Needleman (1995)] Tvergaard V. and Needleman A., 1995. “Effects of Nonlocal Damage in Porous Plastic Solids”, *Int. J. Solids Structures*, **32**, 1063-1077.
- [Rousselier (1981)] G. Rousselier, 1981. “Finite Deformation Constitutive Relations and Ductile Fracture,” Edited by Nemat-Nasser, North-Holland, Amsterdam, pp. 201-217.
- [Yamaguchi et al. (1992)] Yamaguchi, K., Ueda, S., Jan, F.S., Takakura, N., 1992. “Effects of Strain Rate and Temperature on Deformation Resistance of Stainless Steel,” *Mechanical Behavior of Materials-VI*, vol. 3, Headington Hill Hall, Pergamon Press, Oxford, pp. 805-810.
- [Zukas (1990)] Zukas, J.A., Editor 1990. “High Velocity Impact Dynamic,” John Wiley Son, Inc. New York.